Mobile bank conditions for laminar microrivers

Olivier Devauchelle, Christophe Josserand, Pierre-Yves Lagrée, Stéphane Zaleski

Mobile Bank Conditions for Laminar Micro-Rivers

Olivier Devauchelle,[*] Christophe Josserand,[†] Pierre-Yves Lagrée[†] and Stéphane Zaleski[†]

February 29, 2008

Abstract

The present study aims to establish a simple mechanistic model for river bank erosion. Recent experiments demonstrate that small-scale laminar flumes can develop erosion structures similar to those encountered in Nature. From Saint-Venant's Equations, a classical sediment transport law and a simple avalanche model, it is shown that bank failure caused by flow erosion can be represented through simple boundary conditions. These conditions are able to deal with the water level adjustment imposed by a constant water outflow condition. Finally, they are implemented to approach numerically the widening of a laminar river. Keywords: river morphology, bank erosion, bedload transport, micro scale experiment

Résumé

La présente étude se donne pour objectif d'établir un modèle simple de berge érodable. De récentes contributions ont démontré expérimentalement que dans des micro-rivières de laboratoire, parcourues par un écoulement laminaire, l'érosion peut produire des structures similaires à celles observées en milieu naturel. Les équations de Saint-Venant en régime laminaire associées à une loi de transport sédimentaire classique ainsi qu'à un modèle simplifié d'avalanche, permettent de déterminer un ensemble de conditions aux limites décrivant l'effondrement des berges sous l'effet de l'érosion, et capables de prendre en compte des variations du niveau de l'eau de l'écoulement. Cette dernière propriété est indispensable si l'on souhaite imposer le débit total de la rivière. Enfin, ces conditions sont mises en œuvres dans le cas d'une micro-rivière rectiligne qui s'élargit sous l'effet de l'érosion. Mots-clefs: morphologie fluviale, érosion des berges, charriage, micro-rivières

1 Introduction

Saint-Venant's equations, when associated to a sediment transport law, are able to represent various river patterns formation as fluid-structure instabilities. The most obvious example is alternate bars development in straight channel [3, 11]. The same bar instability is also responsible, at first order, for the formation of braided patterns [10, 22]. A close relationship between bar instability and meanders formation was soon suggested, and both phenomena where even hardly distinguished in the early contributions [3, 22, 12]. However, to investigate this relationship quantitatively, one need to add a crucial ingredient into the model, namely a bank erosion law.

To our knowledge, the first breakthroughs in this direction were performed by [16] and [2]. Both contributions use a heuristic bank erosion law, according to which the normal velocity of the bank is a continuous function of the water velocity near the bank. The introduction of moving banks into two-dimensional river models allowed to reproduce accurately meanders wavelength, and shed light on the *bend instability* mechanism [2]. However, the heuristic bank erosion law presents serious drawbacks. First, it has not been yet derived from a quantitative bank model, and thus lacks theoretical support. In particular, it does not conserve sediment mass. But the major issue probably consists in its too simple formulation. Indeed, the mech-

[*]Institut de Physique du Globe de Paris, France, devauchelle@ipgp.jussieu.fr

[†]Institut Jean Le Rond d'Alembert, Université Pierre et Marie Curie, France

anisms leading to bank recess (undermining, bank failure) differ from bank advance processes (deposition, vegetation growth, *etc.*). Thus a bank erosion law is very unlikely continuous, and instead should present a sharp transition when the bank normal velocity changes sign. In addition, there is no reason to believe that this law is a function of the mean water velocity only. It is *a priori* a function of every other model quantities, say water depth or bank height at least.

Since the contributions of [16] and [2], attempts to derive bank erosion laws where not common. Among them are the works of [18], and more recently [6, 7]. The later succeeded in numerically implementing complex bank erosion laws designed to take various phenomena into account (bed degradation, lateral erosion, bank collapse). Although [9] demonstrate the ability of their two-dimensional model to reproduce river meandering, the complexity of bank erosion laws pleads for a simplified analysis in the case of straight rivers, where remains only the transverse coordinate. This configuration also presents its own interest: the question of river width selection has been the subject of abundant research [13, 23, 24]. As a consequence, laboratory experiments were performed, and provide straight river widening data [14, 15, 19].

The present study aims to derive one-dimensional erosion law for a laminar flume on non-cohesive granular material, by mean of a simplified but mechanistic approach. Our motivation is based on recent works tending to demonstrate that laminar flows may generate erosion patterns comparable to those encountered in Nature. This is true for rivers [26, 21, 8], but also for submarine canyons [20]. Indeed, the shallow-water equations in laminar regime used here differ from the classical turbulent ones only by the value of a constant coefficient and friction term [8]. The main advantage in considering laminar flows is experimental: experiments involving laminar flumes of centimetric width are much easily performed than their turbulent counterpart.

This paper is organized as follow: a first section is devoted to a general two-dimensionnal model for erosion by laminar flows. Then the simple case of a rectilinear river is studied, which limitations call for the bank model presented in the next section. Finally, bank conditions are numerically implemented to represent the widening of a laminar river at constant water discharge.

2 Two-dimensional laminar flow and erosion

2.1 Saint-Venant equations for the flow

Experimental laminar flumes generally imply shallow flows. Their typical depth is about 5 mm, whereas their width and length are of the order of 10 cm and 1 m respectively [21]. Consequently, the effects of vertical water velocity may be neglected. Laminar Saint-Venant's equations result from the vertical integration of Navier-Stokes equations, under the assumption that a parabola fits the vertical velocity profile (Nußelt film).

In addition, we hereafter assume that the flow characteristic time is much smaller than erosion time. This is a common hypothesis in Geomorphology [22]. It allows one to neglect the time derivative in the flow equations. The momentum conservation then reads

$$\frac{6}{5}F^2 u_l \partial_l u_i = S\delta_{i,1} - \partial_i \eta - S\frac{u_i}{d^2}, \qquad (1)$$

where $\mathbf{u}$, F, S, η and d denote the vertically averaged water velocity, the Froude number, the mean slope of the plane, the water surface elevation and the flow depth respectively. These quantities were made non-dimensional, by mean of typical velocity $\mathcal{U}$ and typical depth $\mathcal{H}$. The Froude number is then $F = \mathcal{U}/\sqrt{g\mathcal{H}}$. In the following, x and y are the mean slope and transverse directions (see figure 1).

As momentum equations, the water mass conservation equation can be vertically integrated. This procedure leads to

$$\partial_l (du_l) = 0. \qquad (2)$$

From the solution of equations (1) and (2), one can deduce the shear stress $\boldsymbol{\tau}$ exerted by the stationnary flow: $\tau_i = u_i/d$.

2.2 Sediment transport equations

2.2.1 Exner's equation

If the sediment particles are large and dense enough, their settling velocity comparable to, or larger to, the water velocity. In that case, they remain at the river bed surface, and flow transports them as bedload [4]. The latest is the dominant flow-induced

transport in most experimental flumes, where suspension is negligible. Then, the bed topography evolution can be determined by means of Exner's equation, which renders the sediment mass conservation:

$$\partial_t h + \partial_l q_l = 0, \tag{3}$$

where $\mathbf{q}$ denotes the horizontal sediment transport flux per unit length.

Bedload transport is induced by two forces: the tangential stress exerted by the flow, and gravity. A complete transport law should combine both effects [18, 17]. However, for the sake of simplicity, we will hereafter separate these effects. We assume that the total sediment flux is the sum of an avalanche flux, independant from the flow, and an erosion flux induced by the shear stress $\boldsymbol{\tau}$. Then

$$\mathbf{q} = \mathbf{q}_e + \frac{1}{\epsilon}\mathbf{q}_a, \tag{4}$$

where $\mathbf{q}_e$ and $\mathbf{q}_a$ denote the erosion and avalanche sediment fluxes respectively. The small non-dimensional parameter ϵ indicates that avalanches occur at short time scales, as compared to erosion (see section 2.2.3).

2.2.2   Erosion by water

Numerous bedload models can be found in the literature [25]. For moderate bottom slope, most models may be expressed as follow:

$$q_{e,i} = \phi(\theta)\left(\frac{u_i}{\|\mathbf{u}\|} - \gamma\partial_i h\right), \tag{5}$$

where $\theta = \rho\nu\|\boldsymbol{\tau}\|/(\rho_s - \rho)d_s$ is the Shields parameter, and γ a constant of order one. The quantities ρ, ρ_s, ν and d_s denote water and sediment densities, water viscosity and the mean diameter of sediment grains. The shape of function ϕ itself is the subject of intense research (see [5] among others), but it obviously vanishes at the origin. it is generally accepted that it is a positive, growing and convex function. The main question about ϕ concerns the existence of a threshold, below which no grain moves. The analysis presented below (excepted the illustrative case of section 3.1) holds for any erosion law ϕ, provided it presents the main features above mentioned. To the contrary, the hypothesis stating that the sediment flux remains at equilibrium with bottom shear stress [5] is essential to the present study. For illustrative purpose, we will set $\phi = \theta^\beta$ with $\beta = 3.75$.

2.2.3   Avalanches

A complete dynamical model for granular flows is far beyond the scope of the present study. In order to take the effects of avalanches into account, we use a simple heuristic model, proposed by [1] to model the downwind side of eolian dunes.

In non-cohesive granular materials, avalanches are intermittent phenomena, occurring only if the surface slope exceeds a critical angle denoted α_c. Above this threshold, the grains flux is a growing function of the excess slope:

$$q_{a,i} = \varphi\left(\|\nabla h\|\right)\frac{\partial_i h}{\|\nabla h\|}, \tag{6}$$

where φ vanishes below α_c.

In the general case, the system formed by the above equations cannot be solved easily, even numerically, due to the large time scale separation between avalanches and erosion. Instead, one can take advantage of the small value of ϵ to derive integral conditions describing avalanches. It is the purpose of the following developments.

3   Laminar flume widening

3.1   A simple case: no avalanche and constant water level

In a first attempt to evaluate some solutions of the above erosion model, one may consider a straight river. Since the flume cross-section is invariant with respect to any translation in the flow direction (that is, x), the full problem reduces to one dimensional equations, where only y and t remain. Saint-Venant's equations (1) and (2) then read $\theta = \theta_* d$ and $\theta_* = \rho g S \mathcal{H}/(\rho_s - \rho)d_s$. In the same way, Exner's equation becomes

$$\partial_t h = -\partial_y q, \quad q = q_e + \frac{1}{\epsilon}q_a, \tag{7}$$

where the sediment fluxes are

$$q_e = -\gamma\phi(\theta_* d)\partial_y h, \tag{8}$$

$$q_a = -\varphi\left(|\partial_y h|\right)\mathrm{sign}(\partial_y h). \tag{9}$$

If one assumes that no avalanche occurs, and represents the erosion function by a power-law ($\phi(\theta) = \theta^\beta$), then a simple analytical solution can be derived [8]:

$$h = -\frac{1}{t^{1/(\beta+2)}}\left(A - \frac{\beta y^2}{2(\beta+2)t^{2/(\beta+2)}}\right)^{1/\beta}, \tag{10}$$

where A is a constant linked to the river section area. This solution is valid only if $\eta = 0$ at any time.

This solution illustrates the limitations of a model without avalanches. Indeed, for $\beta > 1$ (this is usually the case in the literature), the bed transverse slope $\partial_y h$ diverges at the bank (that is, for $h = 0$). For non-cohesive sediment, such steepness triggers avalanches. Consequently, there must be a domain in the bank neighbourhood where avalanches occur. This idea inspired the bank model presented in the following section.

3.2   Non-cohesive bank conditions

3.2.1   Model description

A realistic non-cohesive bank model should describe the effect of avalanches that undermine the bank foot. It should also be able to take water level variations into account, so that the total water outflow Q can remain constant (see section 3.3.1). The simplest way to do so is to assume that avalanches are contained at the bank foot, as on figure 1. Mathematically, we define a point a as follow:

$$\partial_y h \begin{cases} < \alpha_c & \text{on} \quad [0, a[\\ \geq \alpha_c & \text{on} \quad [a, b] \end{cases} \tag{11}$$

The bank height is represented by a discontinuity of the topography h at point b where the flume depth vanishes. This assumption corresponds to experimental flumes behaviour. Above the water level, sediments are wet but unsaturated. Capillarity then introduces the cohesion necessary to support vertical banks.

Finally, for the sake of simplicity, the sediment topography out of the river bed is assumed to be uniform, and arbitrarily set to zero.

3.2.2   Boundary conditions

Boundary conditions at point a rest on the continuity of both sediment flux and bed topography. The first comes from the sediment mass conservation, the second from the absence of cohesion in the fully saturated sediment. These statements read

$$h(a(t), t) = h_-(t), \tag{12}$$

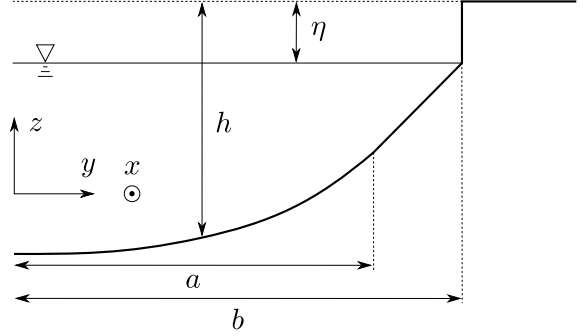$$q(a(t), t) = q_-(t), \tag{13}$$

Figure 1: Simplified scheme of a micro-river bank, and associated notations. By definition, avalanches occur only between point a and point b.

where h_- and q_- denote the limit values of h and q at the left-hand side of point a. Both are function of time only.

Point b refers to the intersection of the water surface with the topography, thus

$$h(b(t), t) = \eta. \tag{14}$$

The sediment mass conservation at point b requires that the flux be the product of the topography discontinuity with the velocity of the point b itself:

$$q(b(t), t) = \eta \dot{b}. \tag{15}$$

Associated to these boundary conditions, equations (7), (8) and (9) can be solved on segment $[a, b]$, provided q_- and h_-.

3.2.3   Asymptotic analysis of the avalanche

Series development   The height of the river bed may be developed as $h = h_0 + \epsilon h_1 + \mathcal{O}(\epsilon^2)$. Similarly, let us define $q_{e,0}$ and $q_{e,1}$ for the erosion flux, $q_{a,0}$ and $q_{a,1}$ for the avalanche flux and b_0 and b_1 for the bank position. To zeroth order, the flux boundary condition (13) gives

$$q_{a,0} = 0, \quad q_{e,0} + q_{a,1} = q_-, \tag{16}$$

for $y = a$. In the same way, the boundary conditions (12), (14) and (15) lead respectively to

$$h_0 = h_-, \quad h_1 = 0 \quad \text{for} \quad y = a, \tag{17}$$

$$h_0|_{b_0} = \eta, \quad h_1|_{b_0} + b_1 (\partial_y h_0)|_{b_0} = 0, \tag{18}$$

4

$$q_{a,0}|_{b_0} = 0,$$

$$\eta \dot{b}_0 = q_{e,0}|_{b_0} + q_{a,1}|_{b_0} + b_1(\partial_y q_{a,0})|_{b_0}. \quad (19)$$

Finally, imposing the definition of point a (11) requires that

$$\partial_y h_0 \geq \alpha_c, \quad \partial_y h_1 \geq 0. \quad (20)$$

First integration of Exner's equation At order $1/\epsilon$, Exner's equation (7) reads

$$\partial_y q_{a,0} = 0 \quad (21)$$

for any y on $[a, b]$. Boundary conditions (16) and (19) then lead to $q_{a,0} = 0$ on $[a, b]$. Now, the avalanche flux expression (9) leads to $q_{a,0} = -\varphi(\partial_y h_0)$. Given the avalanche law φ and relation (20), one can impose a vanishing flux $q_{a,0}$ only by setting $\partial_y h_0 = \alpha_c$. Finally, the topography profile at zeroth order is solved, taking the boundary condition (17) into account: $h_0 = \alpha_c(y - a) + h_-$. The boundary condition (18) at the bank foot then impose the geometrical bank relation

$$\alpha_c(b_0 - a) = \eta - h_-. \quad (22)$$

Second integration The bank relation (22) does not provide enough constraints. Fortunately, the following order of our development is easily reached. Exner's equation (7) imposes $\partial_t h_0 = -\partial_y q_{e,0} - \partial_y q_{a,1}$. Taking the boundary condition (16) into account, this equation can be integrated into

$$q_{a,1} = (y - a)\left(\alpha_c \dot{a} - \dot{h}_-\right) - q_{e,0} + q_-, \quad (23)$$

reminding that $\dot{a}$ and $\dot{h}_-$ are functions of time only. The flux boundary condition at the bank (19) imposes that

$$\eta \dot{b}_0 = (b_0 - a)\left(\alpha_c \dot{a} - \dot{h}_-\right) + q_-, \quad (24)$$

where the leading order of Exner's equation (21) has been used.

The next step requires the development of the sediment flux expressions (9) and (8) to order one and zero respectively:

$$q_{a,1} = -\partial_y h_1 \varphi'(\alpha_c), \quad (25)$$

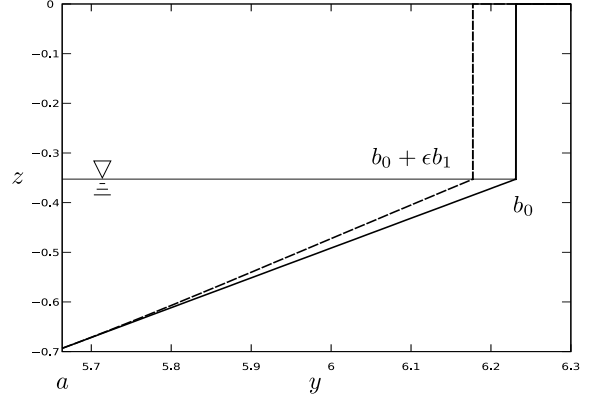$$q_{e,0} = -\gamma \alpha_c \phi(\theta_*(\eta - h_0)). \quad (26)$$

Figure 2: Example of the first order development presented in section 3.2.3. This picture corresponds to time $t = 10$ of the laminar river widening of figure 3. Solid line: h_0; dashed line: $h_0 + \epsilon h_1$. To enhance the effect of order one in the perturbation theory, ϵ is arbitrarily set to 10. In practice, the zeroth order is enough to derive bank boundary condition for the bed evolution equations.

It is then possible to integrate equation (23) from a to any y. This provides an expression for the bed topography at order one:

$$h_1 = -\frac{1}{\varphi'(\alpha_c)}\Big(\frac{1}{2}(y - a)^2(\alpha_c \dot{a} - \dot{h}_-) \\ + (y - a)q_- + \frac{\gamma}{\theta_*}\Big(\Phi(\theta_*(\eta - h_-)) \\ - \Phi(\theta_*(\eta - h_0))\Big)\Big), \quad (27)$$

where Φ refers to the primitive of ϕ which vanishes when its argument does. An example of this order one perturbation is presented on figure 2. Finally, the remaining boundary condition (18) fixes the position b_1 of the bank foot at order one.

Slope boundary condition As long as the river widens, sediments are transported from the bank toward the bed, that is, $q_- \leq 0$. Since, by definition, no avalanche occurs on $[0, a]$, q_- is due to erosion only, and

$$q_- = -\gamma \phi(\theta_* d_-)\partial_y h_- \quad (28)$$

Its minimum value is then $q_- \geq -\gamma \phi(\theta_* d_-)\alpha_c = q_{e,0}|_a$. From boundary condition (16) we then deduce that $q_{a,1} \geq 0$, which can be satisfied only if

5

$q_{a,1} = 0$. In other words, the sediment flux due to avalanches vanishes at $y = a$. Consequently, relations (28) and (16) lead to the following boundary condition:

$$\partial_y h_- = \alpha_c. \qquad (29)$$

Self-consistency of the development The bank model presented here requires that the topography slope $\partial_y h$ remains above the avalanche angle on $[a, b]$. At order one, inequality (20) must be satisfied. Rewriting equation (23) by means of relation (25), the previous inequality reads $f(y) \equiv (y-a)\left(\alpha_c \dot{a} - \dot{h}_-\right) - q_{e,0} + q_- \leq 0$. Indeed, whatever the avalanche law φ, the sediment flux increases with the topography slope, and thus the quantity $\varphi'(\alpha_c)$ is positive. We will see hereafter that f is indeed negative on $[a, b_0]$, provided very general hypothesis on the sediment transport laws.

The second derivative of f reads $\gamma \alpha_c^3 \phi''(\theta(\eta - h_0))$, and thus remains positive. Consequently, the first derivative f' is a growing function. Its value in b_0 is $f'(b_0) = \alpha_c \dot{a} - \dot{h}_- - \gamma \alpha_c^2 \phi'(\theta(\eta - h_0))$. We may assume that the derivative of the erosion law ϕ vanishes for vanishing Shields parameter. Also, for wide rivers (see section 3.3), $\dot{a} \gg \dot{h}_-$ and $f'(b_0)$ is positive.

The sign of f' in a is not obvious. However, it will be shown below that the sign of f' must change on $[a, b_0]$, thus $f'(a)$ must be negative.

Consequently, the variations of f are the following: $f(a) = 0$, then f decreases until it reaches a minimum, then increases up to $f(b_0) = \eta \dot{b}_0$. For a widening river, $\dot{b}_0$ is positive, whereas η is negative. Thus $f(b_0)$ remains negative, proving both that f' must change sign as assumed above, and that f is negative on the whole segment $[a, b_0]$.

3.3 Widening and overflow

3.3.1 Numerical results

The bank model proposed in section 3.2.3 allows us to impose a constant water outflow. Let Q be this outflow:

$$Q \equiv \int_{-\infty}^{\infty} ud \, \mathrm{d}y \approx 2 \int_0^a (\eta - h)^3 \, \mathrm{d}y, \qquad (30)$$

where we have neglected the small amount of water flowing near the bank, through the segment $[a, b]$. By imposing that Q remains constant while the

river widens, we impose a condition that replaces the constant water level imposed in section 3.1.

If we associate the water outflow condition (30) to the boundary conditions (29) and (24), we finally end up with the following system:

$$\begin{cases} \dfrac{\partial h}{\partial t} = -\dfrac{\partial q}{\partial y} \\[2mm] q = -\gamma_n \phi(\theta_*(\eta - h))\dfrac{\partial h}{\partial y} \end{cases} \qquad (31)$$

$$\int_0^a (\eta - h)^3 \, \mathrm{d}y = Q_w, \quad \left.\dfrac{\partial h}{\partial y}\right|_0 = 0, \qquad (32)$$

$$\left.\dfrac{\partial h}{\partial y}\right|_a = \alpha_c, \quad \alpha_c \, q|_a = \eta \dot{\eta} - \left(h\dfrac{\partial h}{\partial t}\right)\Big|_a. \qquad (33)$$

To obtain the above system, the first derivative of the definition $h_- = h(a(t), t)$ has been used.

The solution to this system for a given initial condition can be approached numerically. We employed an explicit finite differences scheme to produce the results presented on figure 3.

Under the effect of erosion and slope-induced sediment diffusion, the laminar river widens and becomes more shallow. Eventually, the water level reaches the bank top, and water overflows. At that point, our model fails.

3.3.2 Sediment mass and water outflow constraints

The river overflow described above can be understood in a simple way. Bank erosion tends to widen the bed. However, due to the river invariance in the main flow (that is x) direction, the sediment mass conservation imposes that the flume section area S be conserved. In other words,

$$S \approx C_1 \mathcal{W} \mathcal{H} \qquad (34)$$

is a constant, where $\mathcal{W}$ and $\mathcal{H}$ respectively stand for the typical width and height of the river. C_1 is a shape constant of order one. Thus widening implies shallowing.

The water outflow Q is also a constant, which may be approached by

$$Q \approx C_2 \mathcal{W}(\eta + H)^3 \qquad (35)$$

for a laminar flow (C_2 is a shape constant). To maintain the outflow to its initial value while the river height decreases, the water level must increase.

Figure 4: Water level of a widening laminar river *vs* its bed width. Solid line: numerical solution (the same as in figure 3); dashed line: simplified relation (36). The conservation of sediment mass and water discharge explains the overflow.
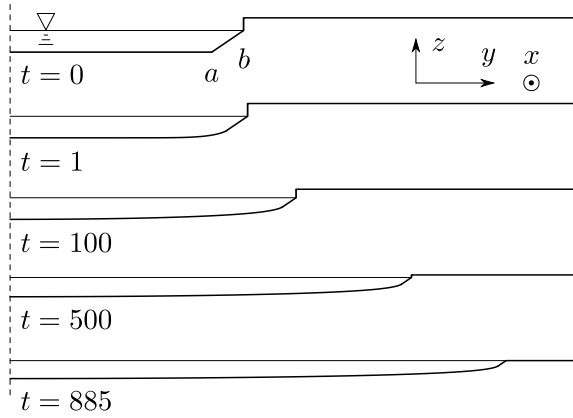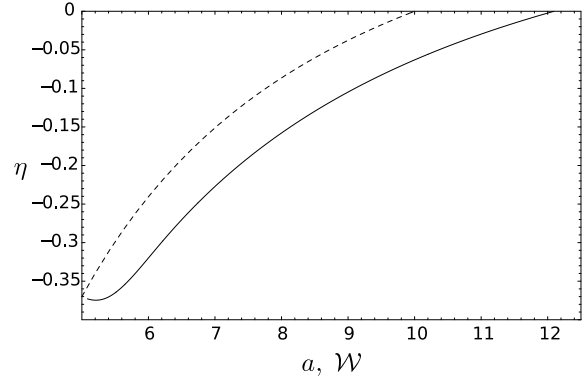
Figure 3: Widening of a straight micro-river, at constant water outflow, using the bank conditions of section 3.2.3. Space scale is arbitrary, but the aspect ratio is preserved. Parameters values are: $\theta_* = 1$, $\alpha_c = 0.6$, $\phi(\theta) = \theta^{3.75}$, $\varphi'(\alpha_c) = 1$. The initial section of the river is a rectangle of width $a = 5$ and depth $h = -1$. The initial water level is $\eta = -0.4$. This level increases as the bed widens, until it reaches the bank height. If the sediment transport law ϕ presents no threshold, water eventually overflows.

From relations (34) and (35), we can express the water level as a function of the river width:

$$\eta \approx \left(\frac{Q}{\mathcal{W}C_2}\right)^{1/3} - \frac{S}{\mathcal{W}C_1}. \qquad (36)$$

In figure 4, the above expression is compared with the numerical solution of figure 3, after setting arbitrarily C_1 and C_2 to one. Even though the two curves differ significantly, the simplified expression (36) reproduces qualitatively the behaviour of the numerical solution. In particular, for very large river ($\mathcal{W} \gg 1$), equation (36) becomes $\eta \approx (Q/\mathcal{W})^{1/3} > 0$, so predicting an overflow. The fact that the numerical solution does not keep a rectangular shape explains the difference between the two curves.

4   Conclusion

Under well established conditions (experimental laminar flumes on non-cohesive sediment), simplified bank conditions may be established. These conditions respect the sediment mass conservation.

They are derived from the basic mechanism that controls bank erosion. If the sediment transport law does not include any threshold, the river bed widens until water overflows.

The model presented in this study is limited to a specific system. However, the method used here is quite general, and can probably be adapted to different situations (cohesive banks, vegetation growth, *etc.*). In addition, it can easily be generalized in two horizontal dimensions, provided the curvature of the bank remains small as compared to the flow depth.

Straight river widening experiments are found in the literature, but most contributions focus on the equilibrium width. Also, to our knowledge, no experiments were performed at low Reynolds number. Comparison with experimental data is the subject of present work.

Acknowledgements

References

[1] B. Andreotti, P. Claudin, and S. Douady. Selection of dune shapes and velocities. part 2: A two-dimensional modelling. *European Physical Journal B*, 2002.

[2] P. Blondeaux and G. Seminara. A unified bar-bend theory of river meanders. *J. Fluid Mech.*, 157:449–470, 1985.

[3] R. A. Callander. Instability and river channels. *J. Fluid Mech.*, 36(3):465–480, 1969.

[4] H. Chanson. *The hydraulics of open channel flow: an introduction*, chapter 6, pages 141–241. Elsevier, 2004.

[5] F. Charru, H. Mouilleron, and O. Eiff. Erosion and deposition of particles on a bed sheared by a viscous flow. *J. Fluid Mech.*, 519:55–80, 2004.

[6] D. Chen and JG Duan. Modeling width adjustment in meandering channels. *Journal of Hydrology*, 321(1-4):59–76, 2006.

[7] S.E. Darby, A.M. Alabyan, and M.J. Van de Wiel. Numerical simulation of bank erosion and channel migration in meandering rivers. *Water Resources Research*, 38(9):1163, 2002.

[8] O. Devauchelle, C. Josserand, P.-Y. Lagre, and S. Zaleski. Morphodynamic modeling of erodible laminar channels. *Physical Review E*, 76:05631, 2007 2007.

[9] G. D. Duan and P. Y. Julien. Numerical simulation of the inception of channel meandering. *Earth surface processes and landforms*, 30:1093–1110, 2005.

[10] F. Engelund and O. Skovgaard. On the origin of meandering and braiding in alluvial streams. *J. Fluid Mech.*, 57(2):289–302, 1973.

[11] B. Federici and G. Seminara. On the convective nature of bar instability. *J. Fluid Mech.*, 487:125–145, 2003.

[12] J. Fredsøe. Meandering and braiding of rivers. *J. Fluid Mech.*, 84(4):609–624, 1978.

[13] R. E. Glover and Florey Q. L. Stable channel profiles. *U.S. Bur. Reclamation, Hydr.*, 325, 1951.

[14] S. Ikeda. Self-formed straight channels in sandy beds. *Journal of Hydraulic Engineering*, 107:389–406, 1981.

[15] S. Ikeda, G. Parker, and Y. Kimura. Stable width and depth of straight gravel rivers with heterogeneous bed materials. *Water Resour. Res.*, 24(5):713–722, 1988.

[16] S. Ikeda, G. Parker, and K. Saway. Bend theory of river meanders. Part 1. Linear development. *J. Fluid Mech.*, 112:363–377, 1981.

[17] C. Josserand, P.-Y. Lagre, and D. Lhuillier. Stationary shear flows of dense granular materials: a tentative continuum modelling. *European Physical Journal*, 14(2):127–135, 2004.

[18] A. Kovacs and G. Parker. A new vectorial bed-load formulation and its application to the time evolution of straight river channels. *J. Fluid Mech.*, 267:153–183, 1994.

[19] G. H. Macky. Large flume experiments on the stable straight gravel bed channel. *Water Resour. Res.*, 35(8), 1999.

[20] F. Metivier, E. Lajeunesse, and M.C. Cacas. Submarine Canyons in the Bathtub, 2005.

[21] F. Mtivier and P. Meunier. Input and Output mass flux correlations in an experimental braided stream. Implications on the dynamics of bed load transport. *Journal of hydrology*, 271:22–38, 2003.

[22] G. Parker. On the cause and characteristic scales of meandering and braiding in rivers. *J. Fluid Mech.*, 76(3):457–480, 1976.

[23] G. Parker. Self-formed straight rivers with equilibrium banks and mobile bed. Part 2. The gravel river. *J. Fluid Mech.*, 89:127–146, 1978.

[24] J. E. Pizzuto. Numerical simulation of gravel river widening. *Water Resour. Res.*, 26(9):1971–1980, 1990.

[25] L. Rijn. Handbook of Sediment Transport by Currents and Waves. *Report H*, 461, 1989.

[26] C. E. Smith. Modeling high sinuosity meanders in a small flume. *Geomorphology*, 25:19–30, 1998.